iScience

CellPress
OPEN ACCESS

Article

Choice-dependent delta-band neural trajectory during semantic category decision making in the human brain

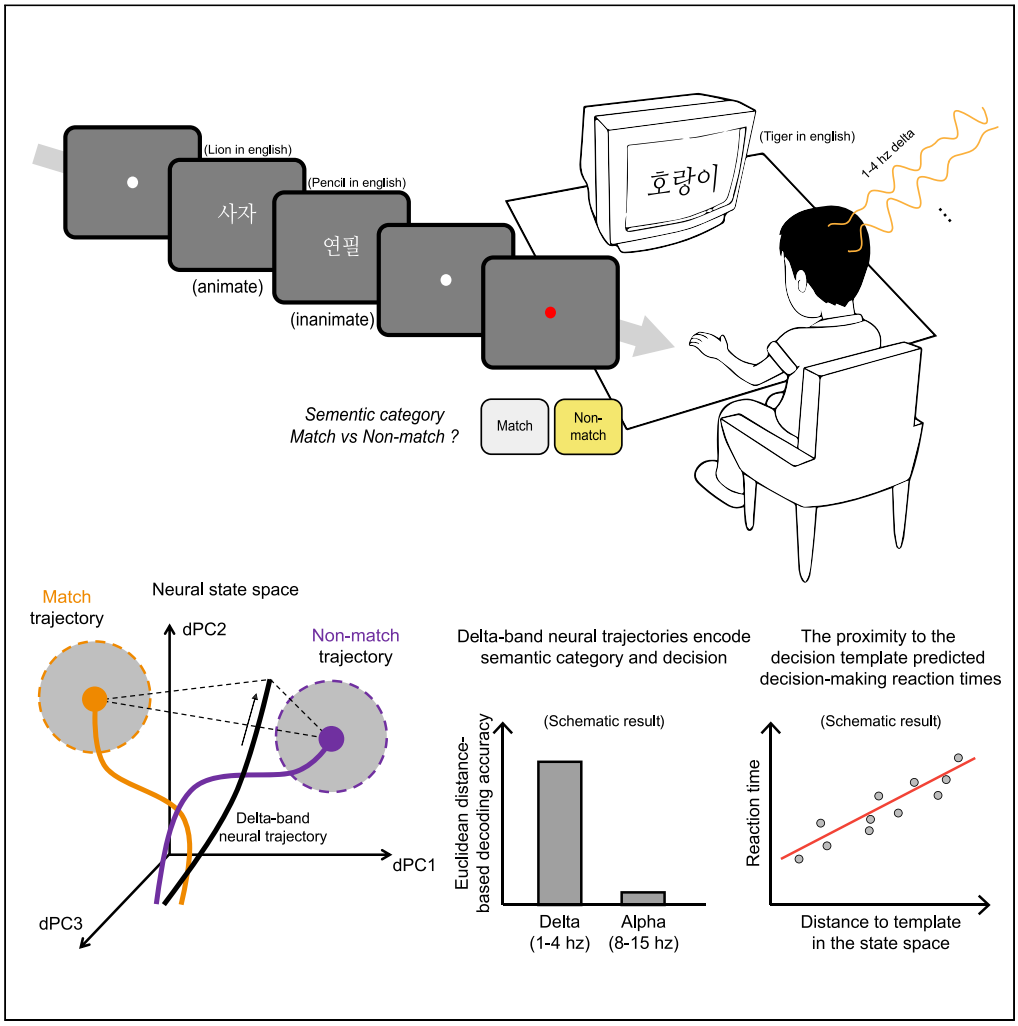

Jongrok Do, Oliver James, Yee-Joon Kim

jongrokdo@ibs.re.kr

Highlights

dPCA of multivariate EEG activities reveals a sequence of semantic decision processes

Distinct delta trajectories emerge based on semantic category and semantic decision

Temporal and posterocentral regions separately encode semantic category and decision

Proximity of neural trajectory to decision template predicts subject's response time

Do et al., iScience 27, 110173
July 19, 2024
https://doi.org/10.1016/j.isci.2024.110173

iScience

CellPress
OPEN ACCESS

Article

Choice-dependent delta-band neural trajectory during semantic category decision making in the human brain

Jongrok Do,[1] Oliver James,[1] and Yee-Joon Kim[1,2,*]

SUMMARY

Recent human brain imaging studies have identified widely distributed cortical areas that represent information about the meaning of language. Yet, the dynamic nature of widespread neural activity as a correlate of the semantic information processing remains poorly explored. Our state space analysis of electroencephalograms (EEGs) recorded during semantic match-to-category task show that depending on the semantic category and decision path chosen by participants, whole-brain delta-band dynamics follow distinct trajectories that are correlated with participants' response time on a trial-by-trial basis. Especially, the proximity of the neural trajectory to category decision-specific region in the state space was predictive of participants' decision-making reaction times. We also found that posterolateral regions primarily encoded word categories while postero-central regions encoded category decisions. Our results demonstrate the role of neural dynamics embedded in the evolving multivariate delta-band activity patterns in processing the semantic relatedness of words and the semantic category-based decision-making.

INTRODUCTION

Humans excel at categorizing stimuli into behaviorally relevant groups and assigning and extracting meaning through both spoken and written language. Multiple brain areas and processes are involved in both categorization and semantic processing. Visual categories are encoded in multiple brain regions in the primate, including the posterior parietal cortex (PPC),[1] prefrontal cortex (PFC),[2,3] and inferotemporal cortex[4,5] with single neuron activity showing distinct responses to stimuli in different categories. Yet, individual neurons in these cortical areas demonstrated mixed, time-varying, and heterogeneous activity patterns during perceptual category-based tasks.[6,7] Thus, to handle this heterogeneity and mixed selectivity, recent studies of perceptual category-based decision making applied dimensionality reduction techniques to population data.[8–10] Techniques such as principal component analysis (PCA) and demixed principal component analysis (dPCA) allowed one to characterize how the sequence of neuronal population responses unfold between subjects' sensory activation and their actions in a compact low-dimensional dynamics of latent signals.

There is also growing evidence that semantic processing is a dynamic process that involves interplay among multiple regions of the brain and a sequence of multiple processing stages.[11] Several fMRI studies have identified widely distributed cortical areas that represent information about the meaning of language.[11–15] These regions, collectively known as the "semantic system," respond more to words than non-words and more to semantic tasks than phonological tasks. The state-of-the-art multivariate decoding of fMRI responses to large-scale semantic feature datasets revealed the cortical semantic maps in which different regions locally encode distinct, interpretable semantic dimensions.[12,16] Although human fMRI imaging studies provided valuable insights on how different brain regions represent various semantic dimensions, many of these studies have not focused on the temporal profiles of semantic information processing. Previous electroencephalogram (EEG) studies have attempted to elucidate the role of delta-band neural activity in language and speech processing.[17,18] According to these studies, there is a debate as to whether delta-band neural oscillations play a critical functional role in syntactic[19–24] or semantic[24–28] processing during language comprehension. However, most of these studies have focused on univariate event-related potentials (ERPs) or oscillatory delta-band responses while participants listened to or watched sentences. Recently, time-generalized multivariate pattern analysis (MVPA) of EEG responses has been applied to EEG in semantic mismatch processing to provide a new perspective that is complimentary to the univariate analysis.[29,30] These studies showed that MVPA revealed an effect of sentence congruency in the later N400–P600 time window while ERPs only showed a robust N400 effect in incongruent sentence. While these MVPA studies have mainly investigated the neural mechanisms underlying semantic mismatch processing, the role of multivariate delta-band neural activities in language processing has not been addressed. Thus, we still lack an understanding of dynamic aspects of the widely distributed delta-band activities in semantic processing,

[1]Center for Cognition and Sociality, Institute for Basic Science, Daejeon 34126, Republic of Korea
[2]Lead contact
*Correspondence: jongrokdo@ibs.re.kr
https://doi.org/10.1016/j.isci.2024.110173

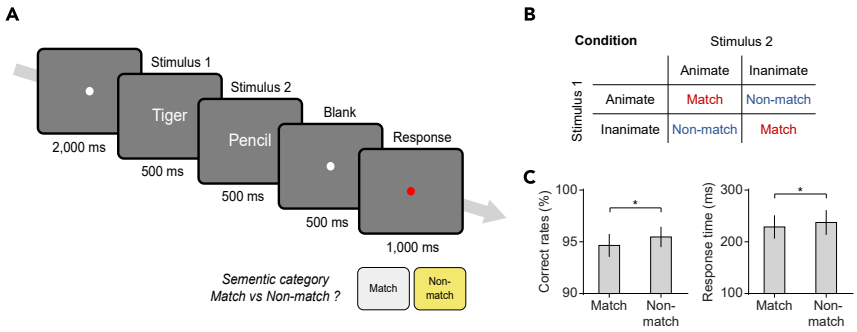

Figure 1. Trial sequence, experimental conditions, and behavioral data analysis

(A) Trial sequence. After a fixation period, two Korean words were sequentially presented, and the participants were instructed to judge whether the two previous words belong to the match or non-match category by pressing 1 (match) or 2 (non-match) button at the end of the sequence.

(B) Experimental conditions. Each trial was one of four combinations of two consecutive words, either animate or inanimate.

(C) Behavioral performance and response time differences between match and non-match semantic category. Error bars indicate ±1 SEM. Asterisk indicates the statistical significance of paired two sample t test ($p < 0.05$).

such as in the perceptual category decision making studies that used the dimension reduction method to visualize the entire process of neural trajectories of perceptual decision making in low-dimensional state space.

Here we investigated the neural trajectories of semantic category-based decision making by applying the dimension reduction technique to multivariate EEG activity recorded from human participants while they performed a simple semantic match-to-category task in which they were asked to judge whether the two consecutive words (animate or inanimate) belonged to the match or non-match category. During the semantic category decision task, the delta-band neural trajectory moved through a low dimensional state space, identifiable via dPCA, in response to participants' semantic processing and their decision choices. At each step of semantic processing, the Euclidean distance-based decoding analysis showed that delta-band neural trajectories in the state space were well separated not only between animate and inanimate word categories but also between match and non-match decisions. We found that posterior and temporal areas were primarily involved in encoding word category information, while postero-central areas were involved in determining whether the two words belonged to the match category or not. We also found that the proximity of the neural trajectory to the categorical decision-specific region of the state space was predictive of the participant's response time. Especially, trial-by-trial correlations between the decoding accuracies and behavioral response times were significant when the two consecutive words belonged to the match category than when they belonged to the non-match category. Taken together, our findings demonstrate a transient delta-band coding dynamics for semantic category decision making in distributed brain regions.

RESULTS

We analyzed scalp EEG signals from 19 human participants as they judged whether two consecutive words belonged to the same category or not (Figure 1A). Participants were informed of the two word category identities during the practice trials before the start of the first experimental session. When the main experimental session began, on each trial, two words were presented sequentially for 500 ms, all of which fall into one of the two semantic category, animate or inanimate, followed by 500 ms blank period. When the central fixation color changed to red, participants were asked to indicate their category decision by pressing either left (match category) or right (non-match category) arrow button. We instructed participants to maintain their fixation at the center of the screen and withhold eye blinks during the 2.5 s period of each trial. The 800 total trials across the eight blocks can be divided into four types of trial based on the categories of two consecutive words (Figure 1B, animate-animate, animate-inanimate, inanimate-animate, and inanimate-inanimate). On average, participants performed significantly better in non-match trials than in match trials (The 1st column of Figure 1C; $t_{18} = -2.48$, $p = 0.02$) and their response time was significantly slower in non-match trials than in match trials (The 2nd column of Figure 1C; $t_{18} = -2.87$, $p = 0.01$). It is possible that participants were more cautious when judging the two presented categories to be different.

Transient neural dynamics during semantic choices

Based on the debate about the role of delta-band activity in speech and language processing[17,18] and previous studies demonstrating the involvement of delta band activity in the modulating the gain of information processing,[19,20,31–33] we mainly focused our MVPA on delta-band neural activities. To examine the temporal evolution of large-scale neural dynamics during semantic match-to-category tasks, we investigated neural trajectories corresponding to behavioral trajectories following three steps of choices in the multi-dimensional state space. A neural state measured by EEG is a point in high-dimensional state space, where each dimension corresponds to the activity of one of all electrodes. As multivariate brain response changes over time, a sequence of neural state at consecutive time points forms a population trajectory through state space. By using dPCA that finds a small subset of orthogonal axes that not only capture the most variance in data but also segregates response variability due to different task variables onto separate axes,[7–10] we visualized neural trajectories of four types of choices

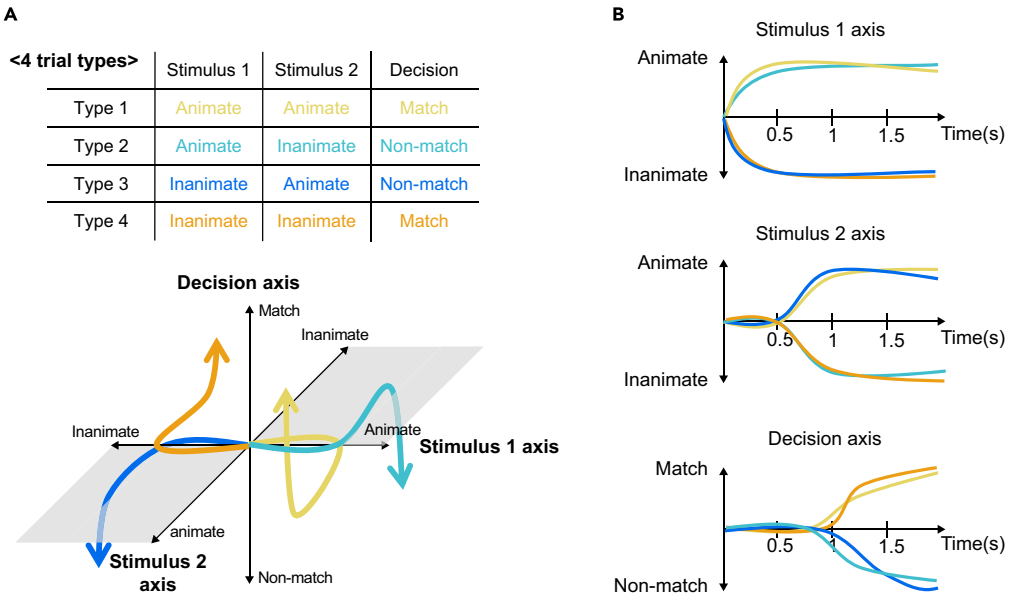

Figure 2. Hypothetical neural trajectories during three sequential processing periods in semantic match-to-category decision making

(A) (Top) Four trial types based on the semantic category combination of the first and second word. (Bottom) Hypothetical neural activity trajectories for four trial types are separately visualized in the three dimensional latent dPC subspace where each axis is defined as the Stimulus 1, Stimulus 2, and Decision by dPCA. (B) Schematic neural trajectories projected onto each task parameter dimension. (Top) Stimulus 1 axis where neural trajectories bifurcate depending on the category of the first word (animate or inanimate) after its presentation. (Middle) Stimulus 2 axis. (Bottom) Decision axis. Line colors indicate four trial types.

in a low-dimensional subspace that is most responsive to task conditions. We extracted five axes for each task variable of interest, amounting to a total of fifteen axes: the first and second axes separating the categories (animate vs. inanimate) of Stimulus 1 and Stimulus 2, respectively, and the third one separating the categories of participants' decisions (match vs. non-match). Figure 2 shows schematic neural trajectories for the four types of choices. The four neural trajectories stay close together along each axis until the corresponding category is selected, and diverge after the choice (Figure 2B). In this study, we defined the state space using the top five dPCs for each task variable that explained 0.46 $\pm$ 0.05% for Stimulus 1, 0.39 $\pm$ 0.03% for Stimulus 2, and 0.41 $\pm$ 0.03% for Decision (mean $\pm$ SEM across participants) of total variance in the data (see Figure S1 for scree plot for each of the dPC variables). Time-varying components account for a substantial portion total variance (the top five dPCs explained 55.85 $\pm$ 3.74%; see Figure S1 for scree plot for each of the dPC variables). All dPCA-based results were computed using the top five dPCs unless otherwise noted. The reported results are robust against the choice of the number of dPCs ranging from 2 up to all EEG channels included.

To quantify how neural trajectories move in state space during semantic match-to-category tasks, we applied a Euclidean distance-based decoding analysis (see STAR Methods for details). The general explanation of our methodology is here. Trials of multivariate neural activities (111 EEG channels space or dimension-reduced space) were divided into training and test sets. Training data were averaged according to the category of the specific task parameter to be decoded, forming templates for each category. For example, to decode for Stimulus 1, the training data are divided into two groups: one where Stimulus 1 was "animate" and the other where Stimulus 1 was "inanimate," and each group was averaged to form an "animate template" and an "inanimate template," respectively. Then, at each time point, we calculated the Euclidean distance from the neural trajectory of test trials to each of the two templates and classified these test trials into the category of the closest template. When we performed this analysis in the low-dimensional state space, training data were used to compute weight matrix for projecting high-dimensional training dataset onto low-dimensional state space and template trajectories were calculated in this dimension-reduced space. Test trials were then projected onto this same space and Euclidean distances to each template were calculated.

We applied a Euclidean distance-based decoding analysis to not only delta-band neural trajectories but also alpha-band neural trajectories as the power spectrum averaged across all 111 electrodes (red circled in Figure 3A inset) and all participants showed alpha-band activity (Figure 3A). First, data were analyzed in each participant's original 111 high-dimensional state space, and statistics were pooled across participants (Figures 3B and 3C). The neural activities of all trials except for incorrect trials were trained and tested in the leave-four-trial-out cross validation procedure (one trial for each of four stimulus combinations, AA, AI, IA, and II; A = animate, I = inanimate) in the state space. The trial-averaged neural trajectory was defined as the template for each category (orange and purple lines in Figure 3B). At each time point, we then calculated the Euclidean distance from the neural trajectory of each of the four left-out trials to each of the two templates and classified this test trial into the category of the closest template (dotted black distances A and B in Figure 3B). Thus, the Euclidean distance-based decoding accuracy indicates the proximity to the category-specific template of the state space at every time and trial. The decoding accuracy was defined as the number of correctly labeled trials divided by the total number of trials. The red lined graph in the left column of Figure 3C

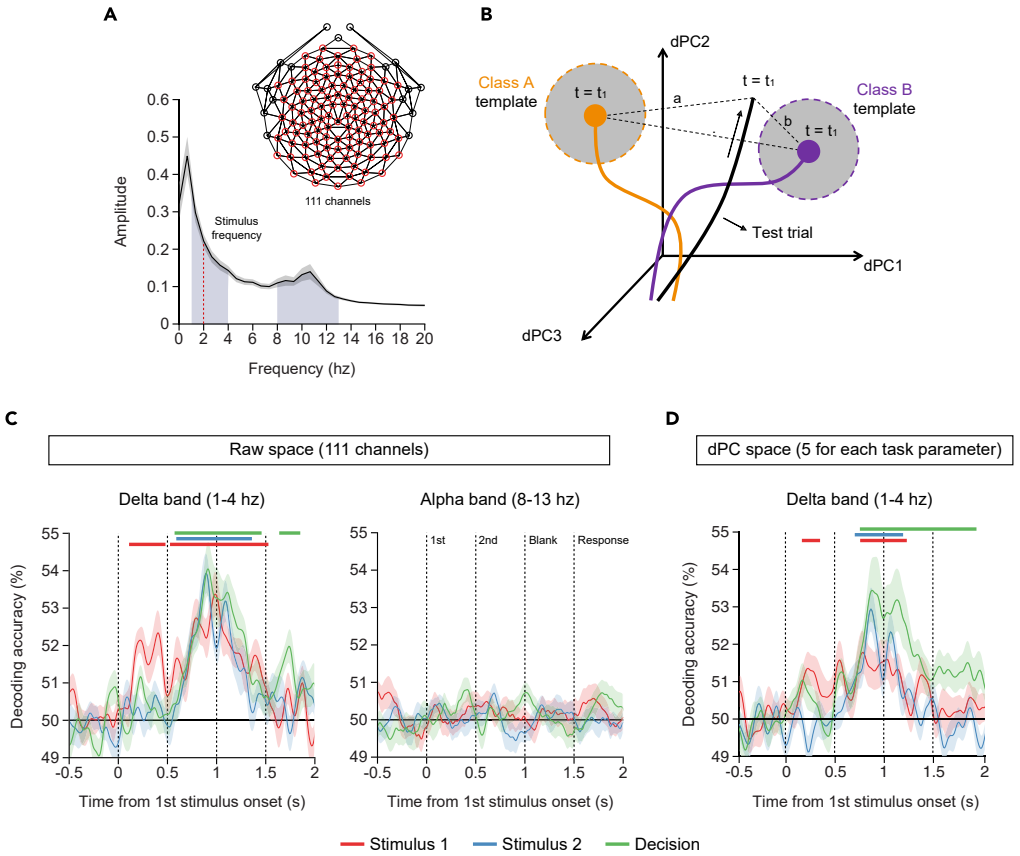

Figure 3. Illustration of Euclidean distance-based decoding analysis and procedure

(A) Power spectrum averaged across 111 electrodes and all participants. The shaded areas indicate two frequencies of interest (delta and alpha). Red dashed line indicates the word presentation rate. Shaded error bars indicate ±1 SEM. Inset: 128-channel EEG recording sites (circled electrodes) and 111 electrodes used for dPCA (red circles).

(B) Schematic of the Euclidean distance-based decoding analysis.

(C) Euclidean distance-based decoding accuracy for delta-band (left column) and alpha-band activity (right column) in original 111 high-dimensional state space.

(D) Euclidean distance-based decoding accuracy for delta-band activity in low-dimensional state space after dPCA was applied. Red, blue, and green line indicates decoding accuracy for each of the three task parameters, the first word category, the second word category, and the semantic decision, respectively. Top bars: the time period when the decoding accuracy is significantly greater than 50% ($p < 0.05$, based on cluster extent). Shaded error bars indicate ±1 SEM.

shows that animate and inanimate trials followed significantly distinct trajectories soon after the first word onset (1st significant cluster: 124–474 ms after the first word onset, cluster-corrected $p = 0.004$, 2nd significant cluster: 520–1512 ms after the first word onset, cluster-corrected $p = 0.002$; see Figure S2 for the results of individual participants). In the same way, we defined both animate and inanimate template of the second word on the second stimulus axis and classified the test trial by checking which template is closer to the test trial at each time point. The blue lined graph in the left column of Figure 3C shows that the neural activity trajectory moves to a template location depending on the category of the second word after its onset (630–1314 ms after the first word onset, cluster corrected $p = 0.002$; see Figure S2 for the results of individual participants). Finally, the neural activity trajectory moves quickly to a decision (match or non-match) template location almost at the same time when neural trajectory encodes the category of the second word (green line in the left column of Figure 3C. 1st significant cluster: 616–1,436 ms after the first word onset, cluster-corrected $p = 0.002$; 2nd significant cluster: 1,614–1,780 ms after the first word onset, cluster-corrected $p = 0.016$; see Figure S2 for the results of individual participants). When we randomly assigned category labels to all 800 trials and then performed a Euclidean distance-based decoding analysis, we found that non-category axes were indeed represented less strongly than the category axes (Figure S3). Note that this shuffle analysis does not directly address the geometry of word representations. We also showed that our decision decoding results were not merely due to the fact that our data were randomly scattered in high-dimensional state space, which could potentially make every pairwise decoding significant along with everything else (Figure S4). For this, a decoder was trained on 400 animate trials of the first word that included 200 match and 200 non-match trials and then was tested on the remaining 400 inanimate trials of the first word that were never used in training the decoder. This analysis demonstrated that the decision representation generalized across conditions, suggesting that the observed significant decision decoding was not due to the random distribution of data in high-dimensional state space.

For activity filtered in the alpha frequency range, the exact same Euclidean distance-based decoding analyses of neural trajectories show that animate vs. inanimate trajectories as well as match vs. non-match trajectories were not significantly separated during the semantic match-to-category tasks (the right column of Figure 3C; see Figure S2 for the results of individual participants). These results demonstrate that the delta-band neural activity trajectory moves through state space in response to participants' semantic processing and their decision choices during the semantic match-to-category tasks.

Next, we applied dPCA to the training dataset of delta-band neural trajectories to compute weight matrix for projecting the high-dimensional training dataset onto the low-dimensional state space (Figure 3D). Note that the test dataset was not involved in any part of dPCA. Figure 3D shows the Euclidean distance-based decoding accuracy in each task parameter's latent dPC subspace. The red lined graph in Figure 3D shows that animate and inanimate trials followed significantly distinct trajectories soon after the first word onset (1st significant cluster: 170–300 ms after the first word onset, cluster-corrected $p = 0.046$, 2nd significant cluster: 750–1,180 ms after the first word onset, cluster-corrected $p = 0.002$; see Figure S2 for the results of individual participants). In the same way, we defined both animate and inanimate template of the second word on the second stimulus axis and classified the test trial by checking which template is closer to the test trial at each time point. The blue lined graph in Figure 3D shows that the neural activity trajectory moves to a template location depending on the category of the second word after its onset (710–1,150 ms after the first word onset, cluster corrected $p = 0.001$; see Figure S2 for the results of individual participants). Finally, the neural activity trajectory moves quickly to a decision (match or non-match) template location almost at the same time when neural trajectory encodes the category of the second word (green line in Figure 3D. 740–1,900 ms after the first word onset, cluster-corrected $p = 0.001$; see Figure S2 for the results of individual participants). Although the significant decoding accuracies were more sustained in high-dimensional state space than in low-dimensional state space, the temporal dynamics of significant decoding accuracies were similar to each other for all three task parameters (the left column of Figures 3C and 3D). When we repeatedly performed the same Euclidean distance-based decoding analysis in the low dimension from 1 to 5 by incrementally increasing the number of dPCs from 1 to 5 for each task parameter, we found that the decoding accuracy increased from one to two dPCs, with no further improvement of the decoding performance beyond two dPCs (Figure S5). This indicates that two dimensions are enough to represent semantic categories and decisions, again confirming that the observed significant decoding was not due to high dimensionality of the neural representation.

Spatial distribution of choice-dependent neural trajectory

We probed topographies of neural trajectories during semantic category decision tasks using searchlight-based analyses (see STAR Methods) in order to examine which brain regions contributed to processing semantic information. At each and every electrode, we performed the same Euclidean distance-based decoding analyses for neural trajectories during successive behavioral choices. Figure 4 shows topographic change of the decoding accuracy at every 250 ms after the first word onset in each task parameter's latent dPC subspace. At 250 ms after the first and the second word onset, posterior and left temporal regions are dominantly involved in encoding each animate or inanimate category information (more red colored regions—top row, the 1st column of Figure 4B; middle row, the 3rd column of Figure 4B; see also Figure S6). Postero-central regions play roles in the decision on whether the two words belong to the match or non-match category from 750 ms to 1,000 ms after the first word onset (dark red colored regions—Bottom row, the 3rd and 4th columns of Figure 4B; see also Figure S6). The involvement of postero-central areas is likely due to the fact that the third step of semantic decision integrates the semantic information of the first two steps into more abstract information.

The proximity of neural trajectory to semantic category decision-specific region is predictive of the response time of the behavioral category decision

Through the Euclidean distance-based decoding analyses, we have shown that the two semantic category-specific neural trajectories such as animate vs. inanimate or match vs. non-match at each step of semantic category processing occupy separate regions of the state space. This result demonstrates that neural trajectory pass through these semantic category specific regions in the order of behavioral choice. As the next step, we tested if the proximity of the neural trajectory to the category specific region of the state space is predictive of the participant's response time. We compared participant's response times with the Euclidean distance from the correct category template trajectory to neural trajectory of individual trial. If the template occupying category-specific region of the state space was related to the underlying neural process that controls semantic category decision-making, neural trajectory proximity of single trial to the category-specific region would be correlated with behavioral response time. Therefore, we calculated the trial-by-trial correlations between the Euclidean distance to the correct category template trajectory and behavioral response times. Specifically, in the low-dimensional latent subspace of each task parameter (Word 1, Word 2, and Decision), we examined whether participants responded faster as the single-trial neural trajectory got closer to the template at every trial and time. The estimated proximity to the match or non-match category-specific template region at the time windows from 500 to 1,000 ms (cluster-corrected $p = 0.004$) and from 1,250 to 1,400 ms (cluster-corrected $p = 0.002$) had predictive power over the participant's response time (Figure 5A; see Figure S7 for the results of individual participants). In the latent subspace of the first and second word, there was no significant trial-by-trial correlation between the proximity to the animate/inanimate template and the response time. These results suggested that the trial-by-trial change in the encoding of semantic category decision information had accompanying changes in the response time of decision making. This implies that the closer the neural trajectory to the categorical decision template, the faster participants responded.

As shown in Figure 1C, the response time was slightly but significantly faster when two consecutive words belonged to the match category than when they belonged to the non-match category. Thus, we examined whether neural trajectories for the decisions to match

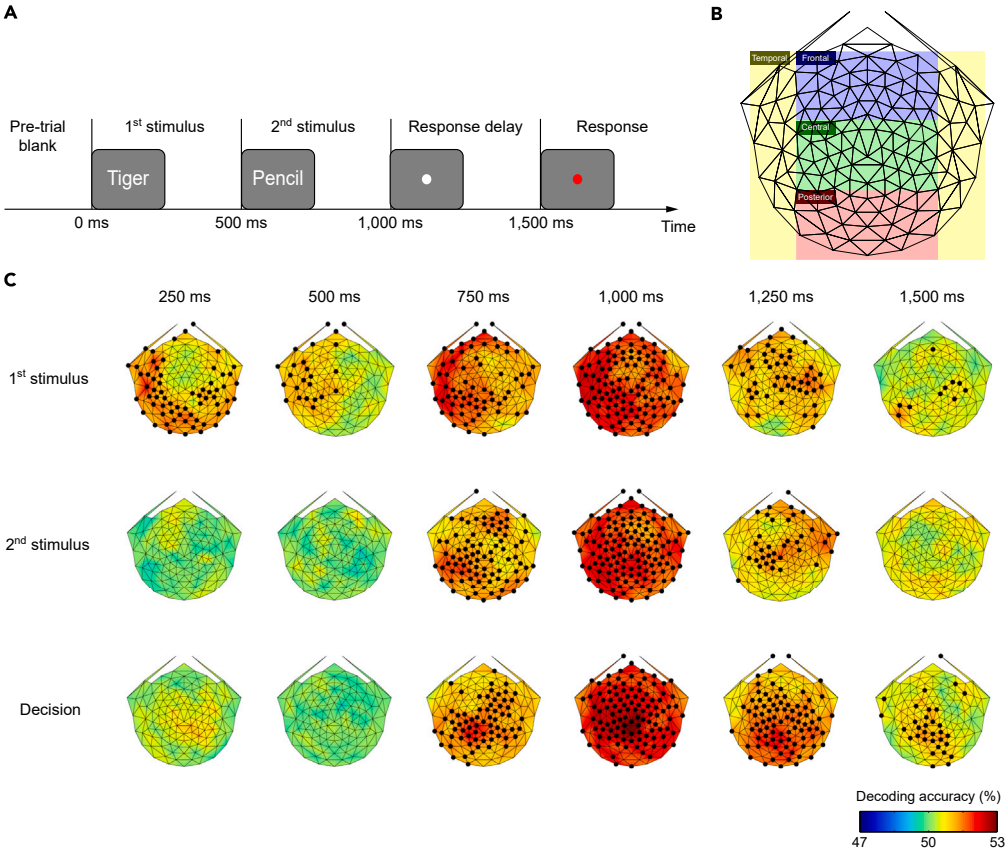

Figure 4. Topographies of Euclidean distance-decoding accuracy for each task parameter over time

(A) Schematic of the trial sequence.

(B) 128-channel electrode layout and electrode clusters corresponding to different brain regions.

(C) Topography of decoding accuracy in each task parameter's latent subspace (top: the first word, middle: the second word, bottom: the decision). Black dots indicate the electrodes where neighboring electrodes showed significant decoding accuracy ($p < 0.01$ based on cluster extent).

and non-match are differentially predictive of behavioral response times. We applied the same trial-by-trial correlation analyses to trials in the match and non-match category, respectively. The estimated proximity to the match category-specific template region at the time windows from 1,440 to 1,770 ms (cluster-corrected $p = 0.005$) and from 690 to 940 ms (cluster-corrected $p = 0.014$) had significant predictive power over the participant's response time (Figure 5B; see Figure S7 for the results of individual participants) for the match category. For the non-match category condition, there was no significant correlation between the participant's response time (Figure 5C; see Figure S7 for the results of individual participants). These results suggest that trial-by-trial correlation between the proximity to the decision category-specific template and the response time is mainly driven by the match category decision.

DISCUSSION

We investigated whether low-dimensional population dynamics of multivariate EEG responses can reliably capture the sequence of processing steps in semantic category decision making. Our results showed that depending on the semantic category and decision path chosen by participants, large-scale slow delta-band cortical dynamics followed distinct trajectories that are correlated with participant's response time on a trial-by-trial basis. At each sequential step of semantic information processing, the delta-band activity trajectories were well separated between animate word category and inanimate word category and between match and non-match decision. Specifically, the proximity of delta-band activity trajectories to category decision-specific region in the latent subspace was predictive of participants' response times to the match category decisions. By contrast, the alpha-band activity trajectories yielded chance-level decoding performance. These findings demonstrate the role of robust transient neural dynamics embedded in the evolving multivariate patterns of slow delta-band activities in processing semantic category decision making.

The observed robust transient delta-band activity dynamics equipped with semantic category-dependent attracting states underlie semantic associative computations in the brain. Although human fMRI imaging studies provided valuable insights on how different brain regions represent various semantic dimensions,[12,14,15] many of these studies have not focused on the temporal profiles of semantic information processing. Our study, however, focuses on the dynamical aspects of semantic category information processing by visualizing the

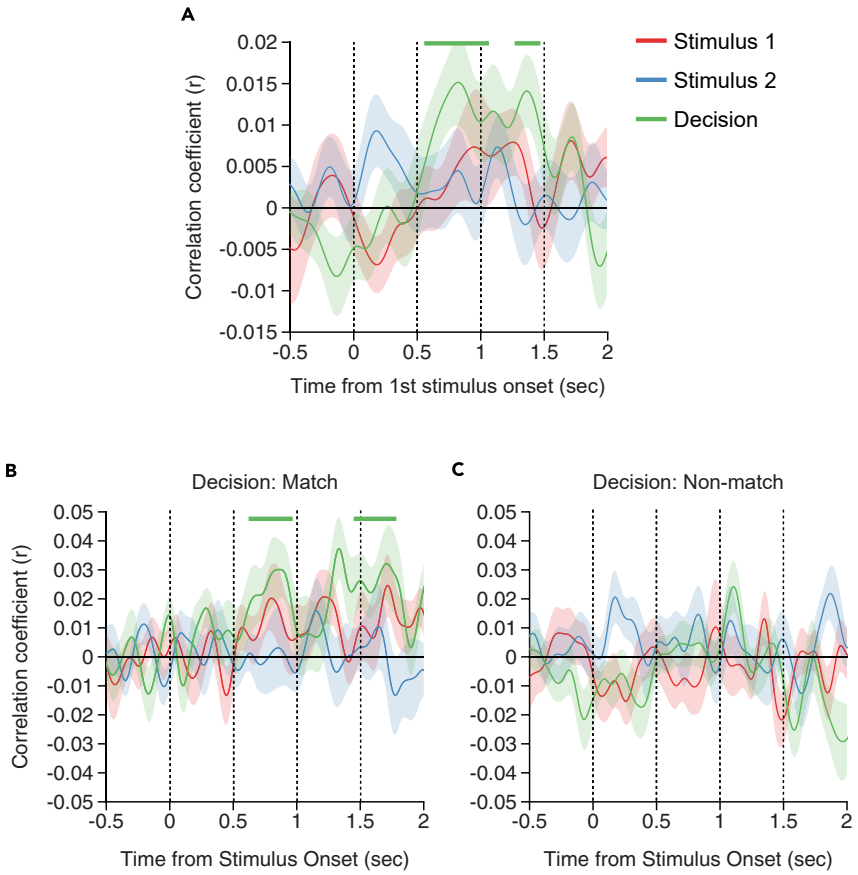

Figure 5. Correlation between neural representation and behavioral response

(A) Pearson correlation coefficient between participants' response time for semantic decision and the neural trajectory's Euclidean distance from category template trajectory in each dPC subspace (Stimulus 1, Stimulus 2, and Decision).

(B and C) The same trial-by-trial correlation analysis applied to trials in the match (B) and non-match (C) category decision. Top bars: the time points when the correlation coefficients were significantly greater than zero ($p < 0.05$, based on cluster extent). Shaded areas indicate ± 1 SEM.

emergences of category-specific and decision-specific clusterings in neural state space. In the context of language processing, delta-band neural tracking has been linked to various aspects of language comprehension, including semantic processing[24–28] and syntactic parsing.[19–24] Recent studies observed stronger delta-band tracking for sentences that followed a predictable rule-based structure, even when the semantic relatedness between words was low, suggesting that delta-band neural tracking primarily reflects hierarchical syntactic structure rather than semantic processing during language comprehension. In these studies, sentence sequences or speeches were presented to participants at the rate of delta frequency, eliciting the oscillatory neural responses at the delta frequency. Thus, slow cortical oscillations entrained to the external stimulation might have served as instruments of attentional selection by modulating rhythmically the gain of information processing in accordance of rhythmic sampling view,[31,32] and were therefore more relevant to syntactic processing rather than semantic processing. Unlike these studies that showed univariate steady-state delta-band neural responses synchronized to stimulus dynamics, there was no significant amplitude increase at the word presentation rate of delta frequency (Figure 3A). In current study, the low-dimensional population dynamics of internal large-scale delta-band neural responses demonstrated distinct neural trajectories depending on the participant's choice of semantic category and decision. This suggests that transient dynamics of delta-band activities moving through the latent state space may be a neural computational mechanism that generates semantic representations and inferences suitable to the immediate task or context.

We further observed that the proximity of neural trajectory to semantic category decision-specific region is predictive of the response time of the behavioral category decision (Figure 5). It is possible that the significant decoding of categorical decision after the second word onset (Figure 3C) might reflect the transformation of match/non-match category information into motor plan for whether to press 1 (match) or 2 (non-match) as shown in previous category-based decision making studies.[34–37] However, the following observed results suggest that these signals reflect changes in how delta-band neural activity patterns encode the categorical decision rather than response selection or motor planning. First, given that the actual button press indicating the choice for match or non-match category did not occur until 1,000 ms after the second word onset, the significant trial-by-trial correlation between the Euclidean distance to the correct decision template trajectory

and behavioral response time around 500 ms immediately after the second word onset suggests that transient neural dynamics at the large-scale network level, embedded in the evolving delta-band activity patterns, underlie semantic category-based decision making. That is, as soon as the second word is presented, decisions about semantic category match or non-match arise from the movement through state space rather than the arrival at a fixed location. Our results are consistent with previous primate and non-primate animal studies showing that transient neural dynamics in local circuits play a critical role in decision making.[7,9,38–40] Second, the fact that the significant correlation between response time and semantic category decision is mainly driven by the match condition (Figures 5B and 5C) strongly suggest that the large-scale delta-band activity trajectory reflects semantic relatedness between the two consecutive words belonged to the match semantic category. The difference in the motor behavior of pressing button 1 (match) and button 2 (non-match) is not so much different that it alone is unlikely to explain the difference in brain-behavior correlations between match and non-match condition. Thus, it is not likely that the representation of match/non-match semantic decision immediately after the second word onset (Figure 3C) is simply a representation of motor action. Finally, if the observed decision decoding was simply a motor action signal, it should have occurred in frontal motor cortical regions. However, the fact that the significant decision decoding dominantly appeared in postero-central area (the bottom row of Figure 4B; red area in the 3rd column and dark red area in the 4th column) also strongly suggests that the observed decision decoding reflects semantic category decision rather than motor action.

It is well established that if a word is preceded by a semantically related word, it is processed faster[41] and its neural response, especially the ERP N400 component and its MEG counterpart, is reduced.[42–44] In the current study, words from the match semantic category are more closely related than words drawn from non-match categories, leading to the faster behavioral response time in match category condition than in non-match category condition (Figure 1C). Our results are likely due to the priming effect, especially the automatic semantic priming effect.[45] Previous studies have identified two kinds of semantic priming, which are automatic and strategic priming.[45] Automatic priming can be caused by, for example, semantic relatedness between words in long-term memory. Strategic priming, however, can actively predict upcoming words based on temporally learned association rules. Because match and non-match trials were randomly ordered in each block, it is difficult for participants to strategically predict the following word in advance. Thus, the fact that the proximity of neural trajectory to the match semantic category decision-specific region is significantly predictive of the behavioral response time might be more based on the semantic relatedness stored in long-term memory rather than on the predictable rule-based syntactic structure. Although previous studies suggest that both syntactic and semantic processing utilize a range of neural oscillations,[17,18] our findings indicate that internal delta-band activities are more closely associated with top-down semantic processes rather than purely syntactic processes.

Future work on semantic fluency task[46–49] (e.g., "name all the animals you can in a minute") will benefit from characterizing the neural activity trajectory of the word retrieval process. When people are asked to retrieve as many members of a category as possible from memory, clusters of semantically related items tend to be retrieved together.[46] This response pattern during the semantic fluency task displayed statistical signatures of memory search that mirror optimal Levy flight foraging in physical space.[46] Levy flight is hypothesized to be optimal strategies for foraging for food in patchy spatial environments, with an individual making a strategic decision to switch away from a cluster of related information as it becomes depleted.[46] Thus, previous study applied this Levy flight foraging hypothesis to a memory search process on semantic network and proposed a model of memory search based on exploration-exploitation tradeoffs known to produce optimal foraging patterns when animal search for food resources.[46] By applying the dimension reduction algorithm such as dPCA and state space analysis in the slow cortical potential range to human M/EEG data recorded during semantic fluency task or word association game, it will allow us to elucidate the dynamic nature of distributed neural activity underlying word retrieval process by measuring if words from the match category are clustered and words from the non-match category are close in the state space. Further, it is important to examine whether or not the large jumps between less related words from non-match category exist as in the Levy flight-like optimal foraging. This will shed new light on neural dynamics governing human memory search on a semantic network.

Limitations of the study

Our analyses and assumptions have some limitations. Although the grand averaged power spectra of EEG during semantic match-to-category task did not show distinctive peak at delta frequency (Figure 2A), we preemptively focused our analyses on delta-band activity based on the recent debate about its role in speech and language processing[17,18] and previous studies demonstrating the involvement of delta band activity in the modulating the gain of information processing.[19,20,31–33] The state space using the top five dPCs of delta-band neural activity pattern also explained only the small proportion of total variance in the data (the values are mentioned at the end of part of Transient neural dynamics during semantic choices in the results section) compared with previous visual perception study where the top five PCs explained >70% variance.[10] This explained variance difference is likely due to the fact that the semantic word stimulus may not stimulate EEG response as much as the visual stimulus that was designed to generate optimal visual response. Nonetheless, current study reliably captures sequences of the large-scale delta-band neural activity pattern evolution over time that corresponds to the participants' choice of the semantic category and the semantic category-based decision. This implies that the widespread endogeneous rather than exogeneous delta-band dynamic network activity underlies the semantic information processing. Our findings significantly further our understanding on the neural mechanisms governing semantic category process and the dynamical nature of distributed neural activity underlying semantic category and semantic category-based decision making. More broadly, the present results will illustrate the utility and potential of probing the dynamical characteristics of spatially distributed brain activity that will provide valuable insights into various perceptual and cognitive processes.

STAR★METHODS

Detailed methods are provided in the online version of this paper and include the following:

- KEY RESOURCES TABLE
- RESOURCES AVAILABILITY
  - Lead contact
  - Materials availability
  - Data and code availability
- EXPERIMENTAL MODEL AND STUDY PARTICIPANT DETAILS
  - Participants
- METHOD DETAILS
  - Stimuli
  - Experimental procedure
  - EEG signal acquisition and preprocessing
  - Power spectrum analysis
  - Demixed Principal Component Analysis (dPCA)
  - Euclidean distance-based decoding analysis
  - Topographies of Euclidean distance-based decoding accuracy for each task parameter
- QUANTIFICATION AND STATISTICAL ANALYSIS

SUPPLEMENTAL INFORMATION

Supplemental information can be found online at https://doi.org/10.1016/j.isci.2024.110173.

ACKNOWLEDGMENTS

This research was supported by Institute for Basic Science (IBS-R001-D2).

AUTHOR CONTRIBUTIONS

Conceptualization: J.D. and Y.-J.K.; methodology: J.D., O.J., and Y.-J.K.; formal analysis: J.D., O.J., and Y.-J.K.; investigation: J.D. and Y.-J.K.; writing – original draft: J.D. and Y.-J.K.; writing – review and editing: J.D., O.J., and Y.-J.K.

DECLARATION OF INTERESTS

The authors declare no competing interests.

Received: December 26, 2023
Revised: April 15, 2024
Accepted: May 31, 2024
Published: June 4, 2024

REFERENCES

1. Freedman, D.J., and Assad, J.A. (2006). Experience-dependent representation of visual categories in parietal cortex. Nature *443*, 85–88.
2. Swaminathan, S.K., and Freedman, D.J. (2012). Preferential encoding of visual categories in parietal cortex compared with prefrontal cortex. Nat. Neurosci. *15*, 315–320.
3. Freedman, D.J., Riesenhuber, M., Poggio, T., and Miller, E.K. (2001). Categorical Representation of Visual Stimuli in the Primate Prefrontal Cortex. Science *291*, 312–316.
4. Freedman, D.J., Riesenhuber, M., Poggio, T., and Miller, E.K. (2003). A Comparison of Primate Prefrontal and Inferior Temporal Cortices during Visual Categorization. J. Neurosci. *23*, 5235–5246.
5. Meyers, E.M., Freedman, D.J., Kreiman, G., Miller, E.K., and Poggio, T. (2008). Dynamic population coding of category information in inferior temporal and prefrontal cortex. J. Neurophysiol. *100*, 1407–1419.
6. Rossi-Pool, R., Zainos, A., Alvarez, M., Zizumbo, J., Vergara, J., and Romo, R. (2017). Decoding a Decision Process in the Neuronal Population of Dorsal Premotor Cortex. Neuron *96*, 1432–1446.e7.
7. Chaisangmongkon, W., Swaminathan, S.K., Freedman, D.J., and Wang, X.J. (2017). Computing by Robust Transience: How the Fronto-Parietal Network Performs Sequential, Category-Based Decisions. Neuron *93*, 1504–1517.e4.
8. Kobak, D., Brendel, W., Constantinidis, C., Feierstein, C.E., Kepecs, A., Mainen, Z.F., Qi, X.L., Romo, R., Uchida, N., and Machens, C.K. (2016). Demixed principal component analysis of neural population data. Elife *5*, e10989.
9. Murray, J.D., Bernacchia, A., Roy, N.A., Constantinidis, C., Romo, R., and Wang, X.-J. (2017). Stable population coding for working memory coexists with heterogeneous neural dynamics in prefrontal cortex. Proc. Natl. Acad. Sci. USA *114*, 394–399.
10. Baria, A.T., Maniscalco, B., and He, B.J. (2017). Initial-state-dependent, robust, transient neural dynamics encode conscious visual perception. PLoS Comput. Biol. *13*, e1005806.
11. Binder, J.R., Desai, R.H., Graves, W.W., and Conant, L.L. (2009). Where is the semantic system? A critical review and meta-analysis of 120 functional neuroimaging studies. Cerebr. Cortex *19*, 2767–2796.
12. Huth, A.G., de Heer, W.A., Griffiths, T.L., Theunissen, F.E., and Gallant, J.L. (2016). Natural speech reveals the semantic maps that tile human cerebral cortex. Nature *532*, 453–458.
13. Ralph, M.A.L., Jefferies, E., Patterson, K., and Rogers, T.T. (2017). The neural and computational bases of semantic cognition. Nat. Rev. Neurosci. *18*, 42–55.

14. Rogers, T.T., and Lambon Ralph, M.A. (2022). Semantic tiles or hub-and-spokes? Trends Cognit. Sci. *26*, 189–190.
15. Popham, S.F., Huth, A.G., Bilenko, N.Y., Deniz, F., Gao, J.S., Nunez-Elizalde, A.O., and Gallant, J.L. (2021). Visual and linguistic semantic representations are aligned at the border of human visual cortex. Nat. Neurosci. *24*, 1628–1636.
16. Huth, A.G., Nishimoto, S., Vu, A.T., and Gallant, J.L. (2012). A continuous semantic space describes the representation of thousands of object and action categories across the human brain. Neuron *76*, 1210–1224.
17. Prystauka, Y., and Lewis, A.G. (2019). The power of neural oscillations to inform sentence comprehension: A linguistic perspective. Lang. Linguist. Compass *13*, e12347.
18. Meyer, L. (2018). The neural oscillations of speech processing and language comprehension: state of the art and emerging mechanisms. Eur. J. Neurosci. *48*, 2609–2621.
19. Lu, Y., Jin, P., Ding, N., and Tian, X. (2023). Delta-band neural tracking primarily reflects rule-based chunking instead of semantic relatedness between words. Cerebr. Cortex *33*, 4448–4458.
20. Lu, Y., Jin, P., Pan, X., and Ding, N. (2022). Delta-band neural activity primarily tracks sentences instead of semantic properties of words. Neuroimage *251*, 118979.
21. Jin, P., Lu, Y., and Ding, N. (2020). Low-frequency neural activity reflects rule-based chunking during speech listening. Elife *9*, e55613.
22. Lo, C.W., Tung, T.Y., Ke, A.H., and Brennan, J.R. (2022). Hierarchy, Not Lexical Regularity, Modulates Low-Frequency Neural Synchrony During Language Comprehension. Neurobiol. Lang. (Camb.) *3*, 538–555.
23. Meyer, L., Henry, M.J., Gaston, P., Schmuck, N., and Friederici, A.D. (2017). Linguistic Bias Modulates Interpretation of Speech via Neural Delta-Band Oscillations. Cerebr. Cortex *27*, 4293–4302.
24. Kielar, A., Panamsky, L., Links, K.A., and Meltzer, J.A. (2015). Localization of electrophysiological responses to semantic and syntactic anomalies in language comprehension with MEG. Neuroimage *105*, 507–524.
25. Brunetti, E., Maldonado, P.E., and Aboitiz, F. (2013). Phase synchronization of delta and theta oscillations increase during the detection of relevant lexical information. Front. Psychol. *4*, 308.
26. Molinaro, N., Lizarazu, M., Lallier, M., Bourguignon, M., and Carreiras, M. (2016). Out-of-synchrony speech entrainment in developmental dyslexia. Hum. Brain Mapp. *37*, 2767–2783.
27. Panda, E.J., Emami, Z., Valiante, T.A., and Pang, E.W. (2021). EEG phase synchronization during semantic unification relates to individual differences in children's vocabulary skill. Dev. Sci. *24*, e12984.
28. Kielar, A., Meltzer, J.A., Moreno, S., Alain, C., and Bialystok, E. (2014). Oscillatory responses to semantic and syntactic violations. J. Cognit. Neurosci. *26*, 2840–2862.
29. Heikel, E., Sassenhagen, J., and Fiebach, C.J. (2018). Time-generalized multivariate analysis of EEG responses reveals a cascading architecture of semantic mismatch processing. Brain Lang. *184*, 43–53.
30. He, Y., Sommer, J., Hansen-Schirra, S., and Nagels, A. (2024). Multivariate pattern analysis of EEG reveals nuanced impact of negation on sentence processing in the N400 and later time windows. Psychophysiology *61*, e14491.
31. Schroeder, C.E., and Lakatos, P. (2009). Low-frequency neuronal oscillations as instruments of sensory selection. Trends Neurosci. *32*, 9–18.
32. Wyart, V., de Gardelle, V., Scholl, J., and Summerfield, C. (2012). Rhythmic fluctuations in evidence accumulation during decision making in the human brain. Neuron *76*, 847–858.
33. Cravo, A.M., Rohenkohl, G., Wyart, V., and Nobre, A.C. (2013). Temporal expectation enhances contrast sensitivity by phase entrainment of low-frequency oscillations in visual cortex. J. Neurosci. *33*, 4002–4010.
34. Zhong, L., Zhang, Y., Duan, C.A., Deng, J., Pan, J., and Xu, N.L. (2019). Causal contributions of parietal cortex to perceptual decision-making during stimulus categorization. Nat. Neurosci. *22*, 963–973.
35. Morcos, A.S., and Harvey, C.D. (2016). History-dependent variability in population dynamics during evidence accumulation in cortex. Nat. Neurosci. *19*, 1672–1681.
36. Driscoll, L.N., Pettit, N.L., Minderer, M., Chettih, S.N., and Harvey, C.D. (2017). Dynamic Reorganization of Neuronal Activity Patterns in Parietal Cortex. Cell *170*, 986–999.e16.
37. Akrami, A., Kopec, C.D., Diamond, M.E., and Brody, C.D. (2018). Posterior parietal cortex represents sensory history and mediates its effects on behaviour. Nature *554*, 368–372.
38. Harvey, C.D., Coen, P., and Tank, D.W. (2012). Choice-specific sequences in parietal cortex during a virtual-navigation decision task. Nature *484*, 62–68.
39. Mazor, O., and Laurent, G. (2005). Transient Dynamics versus Fixed Points in Odor Representations by Locust Antennal Lobe Projection Neurons. Neuron *48*, 661–673.
40. Stokes, M.G., Kusunoki, M., Sigala, N., Nili, H., Gaffan, D., and Duncan, J. (2013). Dynamic Coding for Cognitive Control in Prefrontal Cortex. Neuron *78*, 364–375.
41. Collins, A.M., and Loftus, E.F. (1975). A spreading-activation theory of semantic processing. Psychol. Rev. *82*, 407–428.
42. Broderick, M.P., Anderson, A.J., Di Liberto, G.M., Crosse, M.J., and Lalor, E.C. (2018). Electrophysiological Correlates of Semantic Dissimilarity Reflect the Comprehension of Natural, Narrative Speech. Curr. Biol. *28*, 803–809.e3.
43. Lau, E., Almeida, D., Hines, P.C., and Poeppel, D. (2009). A lexical basis for N400 context effects: Evidence from MEG. Brain Lang. *111*, 161–172.
44. Kutas, M., and Federmeier, K.D. (2011). Thirty years and counting: finding meaning in the N400 component of the event-related brain potential (ERP). Annu. Rev. Psychol. *62*, 621–647.
45. Neely, J.H. (1977). Semantic priming and retrieval from lexical memory: Roles of inhibitionless spreading activation and limited-capacity attention. J. Exp. Psychol. Gen. *106*, 226–254.
46. Hills, T.T., Jones, M.N., and Todd, P.M. (2012). Optimal foraging in semantic memory. Psychol. Rev. *119*, 431–440.
47. Abbott, J.T., Austerweil, J.L., and Griffiths, T.L. (2015). Random walks on semantic networks can resemble optimal foraging. Psychol. Rev. *122*, 558–569.
48. Fathan, M.I., Renfro, E.J., Austerweil, J.L., and Beckage, N.M. (2018). Do Humans Navigate via Random Walks? Modeling Navigation in a Semantic Word Game. Annu. Meet. Cognit. Sci. Soc.
49. Avery, J.E., and Jones, M.N. (2018). Comparing models of semantic fluency: Do humans forage optimally, or walk randomly? In Proceedings of the 40th Annual Meeting of the 40th Annual Meeting of the Cognitive Science Society.
50. Brainard, D.H. (1997). The Psychophysics Toolbox. Spatial Vis. *10*, 433–436.
51. Pelli, D.G. (1997). The VideoToolbox software for visual psychophysics: transforming numbers into movies. Vis. *10*, 437–442.
52. Oostenveld, R., Fries, P., Maris, E., and Schoffelen, J.M. (2011). FieldTrip: Open source software for advanced analysis of MEG, EEG, and invasive electrophysiological data. Comput. Intell. Neurosci. *2011*, 156869.
53. Delorme, A., and Makeig, S. (2004). EEGLAB: an open source toolbox for analysis of single-trial EEG dynamics including independent component analysis. J. Neurosci. Methods *134*, 9–21.
54. Nolan, H., Whelan, R., and Reilly, R.B. (2010). FASTER: Fully Automated Statistical Thresholding for EEG artifact Rejection. J. Neurosci. Methods *192*, 152–162.
55. Behroozi, M., Daliri, M.R., and Shekarchi, B. (2016). EEG phase patterns reflect the representation of semantic categories of objects. Med. Biol. Eng. Comput. *54*, 205–221.
56. Maris, E., and Oostenveld, R. (2007). Nonparametric statistical testing of EEG- and MEG-data. J. Neurosci. Methods *164*, 177–190.

STAR★METHODS

KEY RESOURCES TABLE

REAGENT or RESOURCE	SOURCE	IDENTIFIER
Deposited data		
All preprocessed data and custom MATLAB scripts	This paper	Zenodo: https://doi.org/10.5281/zenodo.11162604
Software and algorithms		
Matlab R2019b	MathWorks	https://kr.mathworks.com/products/matlab.html; RRID:SCR_001622
Psychophysics Toolbox	Brainard (1997)[50] Pelli (1997)[51]	http://psychtoolbox.org/; RRID:SCR_002881
FieldTrip	Oostenveld et al. (2011)[52]	https://www.fieldtriptoolbox.org; RRID:SCR_004849
demixed Principal Component Analysis (dPCA)	Kobak et al. (2016)[8]	https://github.com/machenslab/dPCA
Net Station EEG Software	Electrical Geodesics	https://www.egi.com/research-division/net-station-eeg-software; RRID:SCR_002453
EEGLAB	Delorme and Makeig[53]	https://sccn.ucsd.edu/eeglab/index.php; RRID:SCR_007292
Other		
22″ CRT monitor (ViewSonic PF817)	ViewSonic	https://www.viewsonic.com/us/products/shop/monitors
128-sensor HydroCel Sensor Nets	Electrical Geodesics	https://www.egi.com/research-division/geodesic-sensor-net

RESOURCES AVAILABILITY

Lead contact

Further information and requests for resources should be directed to and will be fulfilled by the Lead contact, Yee-Joon Kim (joon@ibs.re.kr).

Materials availability

This study did not generate new materials.

Data and code availability

- De-identified data, permanently unlinked from all personal identifiable information (PII), were used in the present study. These data are available at Zenodo: https://zenodo.org/records/11162605.
- All analysis codes have been deposited at Zenodo and is publicly available as of the date of publication. DOIs are listed in key resources table.
- Any additional information required to reanalyze the data reported in this paper is available from the lead contact upon request.

EXPERIMENTAL MODEL AND STUDY PARTICIPANT DETAILS

Participants

Nineteen observers (mean age 25.11; six females and thirteen males) participated in the experiment. All observers had normal or corrected-to-normal visual acuity and were fluent in Korean. They gave written consent to participate as paid volunteers, and were tested in a dark room. All observers were naïve to the purpose of the experiment. The study was approved by the Institutional Review Board of the Korea National Institute for Bioethics Policy.

METHOD DETAILS

Stimuli

Visual stimuli were generated and presented using Psychophysics Toolbox[50,51] along with custom scripts written for MATLAB (Mathworks Inc.) running on a Mac mini. The 22″ CRT (ViewSonic PF817) monitor was set to a 100 Hz refresh rate and a resolution of 800 × 600 pixels. Both temporal and luminance calibrations were performed using a calibrated photocell, and monitor gamma tables were adjusted to ensure response linearity and a constant mean luminance of 59 cd/m^2. The observers' viewing distance from the monitor was 70 cm. Korean words from two semantic categories were used: 150 animate and 150 inanimate words. The animate and inanimate words had a similar number of syllables (2.58 vs. 2.78, respectively). Participants viewed two consecutive words written in white against a midgray background.

Experimental procedure

The participants performed a semantic match-to-category task. The participant voluntarily initiated each trial by pressing the space button. A central fixation appeared for 2000 ms and two Korean words were sequentially presented for 500 ms each with no delay period in between (Figure 1A). After the second word disappeared, a white central fixation cue appeared again for 500 ms and then turned red indicating the start of the 1 second response window during which participants were asked to judge whether the two words belong to the match (both animate or inanimate) or non-match (one animate/inanimate and another inanimate/animate) category by pressing 1 button for 'match' and 2 button for 'non-match'. During this entire period of semantic match-to-category task, participants were instructed to maintain fixation on the center of the screen and attempt to withhold eye blinks.

There were four trial types: two semantic categories (animate and inanimate) for both the first and second Korean word. We tested each participant for 800 trials in 8 blocks of 100 trials each. In each block, 50 match and 50 non-match trials were randomly ordered and Korean words were randomly selected among 150 animate and 150 inanimate word sets. We gave participants breaks within and between blocks as necessary.

EEG signal acquisition and preprocessing

The EEG data were recorded with 128-sensor HydroCel Sensor Nets (Electrical Geodesics, Eugene OR) at a sampling rate of 500 Hz and were band-pass filtered from 0.3 Hz to 200 Hz. Offline preprocessing and analysis were performed using Fieldtrip,[52] EEGLAB,[53] and custom scripts in MATLAB (Mathworks Inc.). We used the Fully Automated Statistical Thresholding for EEG Artifact Rejection (FASTER)[54] method for rejecting artifact and interpolating noisy EEG sensors. The EEG was then re-referenced to the common average of all the sensors. The EEG data was epoched from -1000 ms to 2500 ms relative to the onset of the first word stimulus. All analyses except for topographic analysis were performed with 111 EEG channels, excluding 17 channels vulnerable to movement artifacts including electrodes around the ears and on the face. The elimination of these nuisance channels did not change the results of the analyses that used 128 EEG channels. Searchlight-based topographic analysis was performed using 128 channels.

Power spectrum analysis

As previous studies[19,28,55] showed that delta-band neural activity played a functional role in high-level cognitive processing such as categorization and semantics, we examined the population activity in the delta frequency band (1 – 4 Hz). Another reason for focusing our analyses on the delta-band activity was that the stimulus presentation rate was also 2 Hz (500 ms for each word). We also investigated alpha-band activity because power spectrum averaged across electrodes and participants showed a clear bump in alpha band (8 – 13 Hz) activity (Figure 3A). We applied band-pass filter of order 4 to EEG signals to separately extract delta-band and alpha-band activity using a subroutine of Fieldtrip toolbox.[52]

Demixed Principal Component Analysis (dPCA)

To extract population response patterns during the semantic category (animate and inanimate) information processing and categorical decision (match and non-match) making, we applied demixed principal component analysis (dPCA)[8] to multivariate delta-band and alpha-band activities, respectively. We mainly focused dPCA on delta-band activity as its role in speech and language processing has been debated in recent studies of speech and language processing.[19–28] dPCA was developed to compress the data as well as demix the task parameter dependencies on neural activities. To achieve both compression and demixing, additional flexibility was assumed in the loss function of dPCA in that original data was reconstructed from on a distinct encoder axis. The algorithmic and mathematical justification are outlined in Kobak et al. (2016).[8] Major differences in mathematics between PCA and dPCA are summarized below.

First, data matrix X was marginalized over parameters-of-interest (decomposition). Applying it to our task, the original data (neuron x time x trial) was averaged over four task parameters: *Stimulus 1*, *Stimulus 2*, *Decision* (Interaction between *Stimulus 1* and *Stimulus 2*), and *condition-independent* components, and noise term:

$$X = X_{stim1} + X_{stim2} + X_{stim1*2} + X_{time} + X_{noise} = \sum_{\varphi} X_{\varphi} + X_{noise}$$

Second, in a loss term in each parameter φ, a decoder matrix D and an encoder matrix F are separately defined:

$$L_{\varphi} = \|X_{\varphi} - F_{\varphi} D_{\varphi} X\|^2$$

and the loss function is the sum of all individual loss terms of each task parameter:

$$L = \sum_{\varphi} L_{\varphi}$$

Third, matrix F and D are further estimated via singular value decomposition.

The dPCA procedure enables us to visualize neural trajectories in a low-dimensional subspace that is most responsive to task conditions by finding a small set of orthogonal axes that not only capture the most variance in data (like standard PCA), but also segregates response variability due to different task variables onto separate axes. In our case, EEG activity patterns are decomposed into distinct subspaces that

correspond to each task parameter such as semantic category and categorical decision. Three task parameters were used: semantic category for the first and second word (Animate vs. Inanimate) and categorical decision (Match vs. Non-match). The epoched signals were not only baseline corrected by subtracting the average signal from -150 to -50 ms relative to the first word onset but also divided by the standard deviation of the entire signal before performing dPCA analysis. We emphasize that normalization was conducted independently for each trial and electrode to prevent potential leakage, which refers to the improper practice of using the entire dataset's statistics for preprocessing, thereby risking information leakage between training and test sets in the dPCA. Top five principal components for each task parameter plus top five time-varying components were included to constitute low-dimensional subspaces for this task (a total of 20 dimensions). First, the explained variance for these 20 dimensions was calculated using all trials. The top 20 demixed principal components of delta-band activity patterns captured around 57% of the total variance of neural data. To investigate whether each task parameters were reliably represented on the neural subspaces, a distance-based decoding analysis was performed with an assumption that participants would make a decision towards the closer neural trajectory in the corresponding subspaces.

Euclidean distance-based decoding analysis

To more accurately capture the information in temporally dynamically changing EEG patterns, we decided to perform a moving window dPCA analysis with a window size of 500 ms and a window step size of 100 ms. Specifically, the training data (111 channels x 250 time-points x 796 trials after excluding each trial of 4 trial types) were averaged by task conditions (4 trial types; AA, AI, IA, II; A: animate, I: inanimate). Then, the averaged data from training dataset was used to compute weight matrix (transformation matrix bridging high and low dimensions) and was projected on to 20 dimensions (20 dPCs * 250 time-points). We emphasize that the test dataset was not involved in any part of the dimension reduction process. When decoding the category of *Stimulus 1*, *Stimulus 2*, and *Decision*, two trial types are accordingly paired and averaged in the 5 dimensions defined by the dPCA (*Stimulus 1*: AA+AI vs IA+II, *Stimulus 2*: AA+IA vs AI+II, *Decision*: AA+II vs AI+IA), which served as templates (representative trajectories for each category). Then, test trials (4 remaining trials; one trial per trial type) were projected onto the same sub-spaces and Euclidean distance, in five corresponding dimensions for each task parameter, between test trials and two category templates was computed at every time-point ($d_{category\ A}(t)$ and $d_{category\ B}(t)$). The test data was labeled with the class having shorter Euclidean distance among the two category templates (e.g., if a test trial has $d_{category\ A}(t) > d_{category\ B}(t)$, then this trial is labeled as category B). Decoding accuracy was defined as the number of correctly labeled trials divided by the total number of trials. The neural activities of all trials except for incorrect trials were trained and tested in the leave-four-trial-out cross validation procedure (one trial for each of 4 stimulus combinations). These procedures were repeated for every moving window step and overlapping decoding accuracies across moving windows were averaged.

To investigate whether task parameters (semantic category and category decision) were reliably represented in the low-dimensional subspaces, we first conducted an Euclidean distance-based decoding analysis on data without applying any dimension reduction techniques for control (Figure 3C left). In this analysis, all procedures remained unchanged, except that the Euclidean distances were calculated using the intact 111 EEG channel dimension.

To probe whether the degree of proximity to the category template correlates with behavioral measures (response time), we defined "Degree of proximity" at time t as follow:

$$D_{category\ A}(t) = \frac{d_{category\ A}(t)}{d_{category\ A}(t)+d_{category\ B}(t)}$$

$$D_{category\ B}(t) = \frac{d_{category\ B}(t)}{d_{category\ A}(t)+d_{category\ B}(t)}$$

Thus, $D_{category\ A}(t)$ and $D_{category\ B}(t)$ was always in the range between 0 and 1. Test trials with $D_{category\ A}(t)$ of less than 0.5 in a trial with category A presented (or vice-versa) were labeled as a correct classification. We examined if participants make a categorical decision faster when the delta-band neural trajectory approaches closer to the correct template trajectory of the two classes. We calculated Pearson's correlation coefficient between each trial's degree of proximity to the relevant template of either semantic category or semantic decision, $D_{answer\ category}(t)$ and participants' response time.

Topographies of Euclidean distance-based decoding accuracy for each task parameter

To examine the topographic sources of neural trajectories for semantic category and decision over time, we implemented a searchlight-based analyses and calculated a decoding accuracy from each electrode. We used a triangulation method in Fieldtrip[52] to obtain a neighborhood map listing all the neighboring electrodes of every single electrode. Then, we computed neural trajectories of every single neighbor and its Euclidean distance-based decoding accuracy for each task parameter (semantic category and decision). The topography of decoding accuracy was plotted every 250 ms from 250 ms to 1750 ms from the first word onset (Figure 4). Here, we assigned electrode positions to fit the corresponding brain region based on the source-imaged EEG estimation. In estimating cortical current source of the sensor-level EEG signal, it is well known that cortical current sources close to the measuring electrode contribute most to EEG signal at the sensor level. Thus, we divided brain regions as shown in Figure 4 despite the limitation of low spatial resolution of EEG.

QUANTIFICATION AND STATISTICAL ANALYSIS

To correct multiple comparison problem across time points, statistical significance of neural activity was assessed using a non-parametric cluster-based permutation test ($p < 0.05$, 5000 permutations for each test[56]). Significance of electrodes in the topographic plots of Euclidean distance-based decoding accuracy was tested with the same permutation test applied to both time and electrode domain ($p < 0.01$).